UDC 669.295.539.121

STRUCTURE AND MECHANICAL PROPERTIES OF NITRIDE MULTI-LAYER SYSTEMS ON THE BASIS OF HIGH ENTROPY ALLOYS AND TRANSITION METALS OF GROUP VI

U.S. Nyemchenko[1], V.M. Beresnev[1], O.V. Sobol[2], S.V. Lytovchenko[1], V.A. Stolbovoy[3], V.Ju. Novikov[4], A.A. Meylekhov[2], A.A. Postelnyk[2], M.G. Kovaleva[4]

[1]V.N. Karazin Kharkiv National University, Kharkov, Ukraine

E-mail: ululkin@gmail.com;

[2] National Technical University "Kharkiv Polytechnic Institute", Kharkov, Ukraine;

[3]National Science Center "Kharkov Institute of Physics and Technology", Kharkov, Ukraine

[4]Belgorod National Research University, Belgorod, Russia

The influence of technological parameters of obtaining on the possibilities of structural engineering and mechanical properties of multi-layer compositions of the layers of nitrides of high entropy alloy Ti-Zr-Nb-Ta-Hf and of transition metal (Group IV) nitrides has been analysed. It is shown that with the bias potential Ub lesser than -150 V was applied to the substrate during deposition, a two-phase state with the preferred orientation of the crystallites can be reached in multilayer coatings with the thickness of the layers of 50 nm. This leads to high hardness (up to 44 GPa) and to high adhesion strength (critical load up to 125 N) as well as to low wear (with a counterbody Al_2O_3, and with steel Ac100Cr6). High-temperature annealing (700 ^{0}C) of such coatings leads to enhanced texture as a result of atomic ordering, which is accompanied by increasing of hardness up to 59 GPa. The supply of bias potential exceeding 150 V, followed by a substantial mixing at the interphase boundary results in disorientation and improves dispersion of the crystallites, reduces hardness and wear resistance. High temperature annealing of such structures leads to reduction of their mechanical properties.

INTRODUCTION

The last decade is characterized by intensive application of coatings for adjustment of composition, structure, and properties of the surfaces of various products [1 - 9]. The data on relationship between structure and functional properties has become of particular importance with the development of nanotechnologies. Managing the structure on a nanoscale reveals completely new possibilities of fundamental improvement of different functional characteristics of materials and products in many cases [10–12]. To increase the thermal stability of nanomaterials, the concept of multicomponent high entropy alloys (HEA) was proposed relatively recently. According to this concept, which was proved experimentally on a row of compositions [13–16], high entropy of mixing can stabilize formation of a disordered hard solution phase and prevent formation of intermetallic phases during crystallization process. High entropy alloys formed in this way can possess increased strength in combination with good plasticity, oxidation resistance and corrosion [17–18].

Nitrides of high entropy alloys have even higher hardness [17, 19]. But at the same time fragility increases to significant extent and strength of material is, thus, lost. To improve functional properties in this case, a transition to the multilayer compositions with altering layers of nitrides different by composition is effective [1, 20–22]. Nitrides of high entropy alloy Ti-Zr-Nb-Ta-Hf and transition metals of group VI (W or Mo) have been used in this paper s layers.

Using the nitrides of high entropy alloys as layers creates prerequisites for the thermal stability of the obtained material, which is conditioned byt he process of elemental and structural ordering in high entropy multielement alloys at elevated temperatures [23].

The selection of the elements of group VI (W and Mo) as the basis for the second type of nitride layers is caused by the fact that in state of equilibrium mononitrides of these metals are characterized by the formation of phases with non-cubic crystal lattice, which must create an additional barrier to the motion of dislocations at the interphase boundary with HEA nitrides having a cubic lattice and thus reinforcing the material.

EXPERIMENTAL PART

The five-element Ti-Zr-Nb-Ta-Hf cathodes were received by vacuum-arc melting method. To reach a necessary homogeneity of the cathodes they were re-molt for 5–7 times [19]. The deposition of the coatings was carried out with the use of the vacuum-arc installation "Bulat-6" [24]. The deposition was carried out from two cathodes (1 – alloy Ti-Zr-Nb-Ta-Hf, 2 – W or Mo), diametrically opposed to the substrate holder during continuous rotation of the holder, which provides the thickness of each layer of about 50 nm. Steel discs and plates (12X18N9T steel) with the diameter of 45 mm and thickness of 4 mm have been used as a substrate. The annealing of the coatings was carried out during 1 hour in the vacuum furnace VHT 8/22-GR (Nabertherm GmbH) under the pressure of $P = 5\times10^{-6}$ Torr and the temperature of 700^{o}C. In order to study the surface of the multi-component coatings, their elemental composition and distribution of elements on the surface SEM with energy-dispersive spectrometer JSM-6010 LA was used, (JEOL). Measurements of the phase composition of the coatings were carried out using X-ray diffractometer DRON-3M and DRON-4 in the radiation of Cu-K_α

with the use of graphite monochromator in the secondary beam. Registration of scattering was carried out in a discrete shooting mode, with a scanning step, changing in the range $\Delta(2\vartheta) = 0.01...0.05$ depending on the width and intensity of the diffraction lines [25].

Investigation of the coatings for determining adhesive and cohesive strength, resistance to scraping and finding out a mechanism of destruction was carried out with Revetest scratch-tester (CSM Instruments). Scratches were made on the surface of the coating with a help of "Rockwell C" spherical indenter with a rounding radius of 200 μm at continuously increasing load. At the same time the power of acoustic emission, friction coefficient and penetrating depth, as well as the magnitude of normal load (F_N) have been measured. To receive positive results three scratches were made on a surface of each coated sample. The tests were conducted under the following conditions: the load on indenter was increasing from 0.9 to 70 N, sliding sped was 1 mm/min, the length of a scratch – 10 mm, loading speed – 6.91 N/min, frequency of discreteness of a signal 60 Hz, acoustic emission – 9 dB. Measurements of hardness and elasticity modulus of the coatings by means of nanoindentation were performed on the equipment Hysitron TriboIndenter 950 with a diamond Berkovich pyramid (Ti-0039, apex angle 142.3°, radius of the top rounding 100 nm) calibrated by quartz. Maximum load during the measurements was selected in a way to prevent influence of a substrate on the measured quantities. The tribological tests were performed in the atmosphere of air by the scheme "ball – disc". As a friction machine «Tribometer» by CSM Instruments has been used. Samples were the discs from steel 45 (HRC = 55) over the polished surface of which the coatings were deposited (R_a is less than 0.08 μm). The balls of 6.0 mm diameter made of sintered certified materials Al_2O_3 and Ac100Cr6 steel were used as counterbodies. The load during the tests was 3.0 N, sliding speed – 10 cm/s. The tests conform to international standards ASTM G99-959, DIN50324, and ISO 20808. Structure of wear grooves of the coating and wear spots on the balls were studied with use of optical microscope Olympus GX 51 and raster electron microscope FEI Nova NanoSEM 450. Quantitative evaluation of wear resistance of samples and counterbodies was conducted by the wear factor W, the methodology of its calculation is presented in paper [26].

RESULTS AND DISCUSSION

The research of morphology of growth of the multilayer coatings showed their sufficiently large homogeneity and planarity in all the used modes for both types of (TiZrNbTaHf+Mo)N and (TiZrNbTaHf+W)N systems. The drop inhomogenity was revealed on the surface, which did not lead to a significant change in planarity and average thickness (less than 0.5%, see the data on thickness in Fig. 1).

The analysis of element composition (EDX method) has shown that the increase of negative bias potential (U_b) led to depletion of the coating by light atoms. The main reason of this is selective spraying of light atoms during the spraying from the surface of growth [18, 19]. To the largest extent it affects nitrogen atoms, the content of which in the coating with the increase of U_b, in the studied rage decreases more than 1.5 times (Fig. 2).

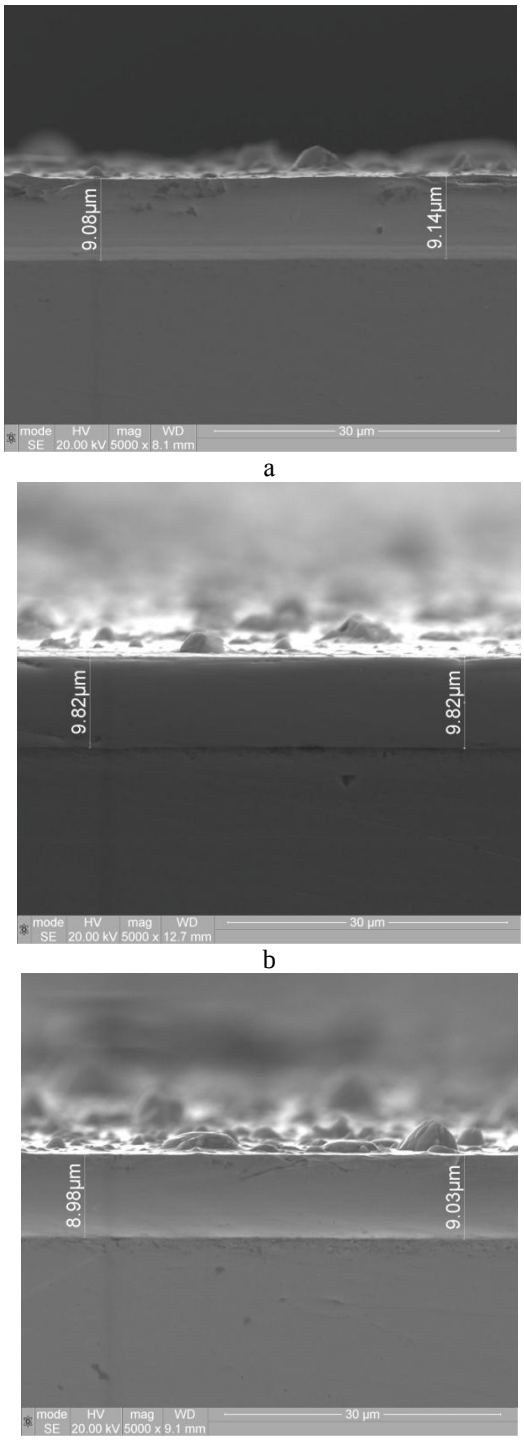

Fig. 1. REM-pictures of the side surface of the "coating – substrate" of the multilayer coatings: a – (TiZrNbTaHf)N/WN (P_N =4×10^{-3} Torr, U_b of -90V), b – (TiZrNbTaHf)N/MoN (P_N =4×10^{-3} Torr, U_b of -50V), c – (TiZrNbTaHf)N/MoN (in (P_N on the =1.5×10^{-3} Torr, U_b) = = -50V)

It is worth noting, that at the same time saturation of the coatings (TiZrNbTaHf)N/WN with nitrogen is larger in comparison with (TiZrNbTaHf)N/MoN by modulus. Also, the spray character (secondary selective spraying) is, apparently, a basis of change of metal components of layers.

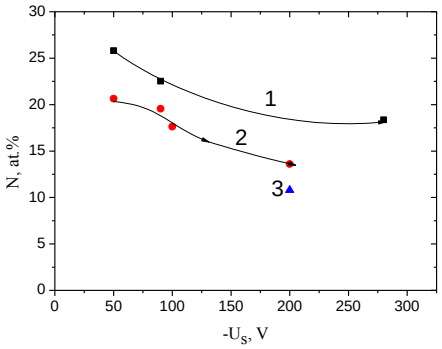

Fig. 2. Dependence of nitrogen atoms contents in the coating on the value of (-U_b).
1 – (TiZrNbTaHf)N/WN (P_N =4·10^{-3} Torr),
2 – (TiZrNbTaHf)N/MoN (P_N = 4·10^{-3} Torr),
3 – (TiZrNbTaHf)N/MoN (P_N =1.5·10^{-3}Torr).

In (TiZrNbTaHf)N/WN coatings in the layers with WN with the increase of U_b from -90 to -280 V the content of heavy W (with respect to the content of metal elements in TiZrNbTaHf layer) increases from 33 to 53%.

For the coatings (TiZrNbTaHf)N/MoN the ratio between the atomic contents of Mo and metal of the second layer (TiZrNbTaHf) with the increase of U_b is practically not observed, remaining at a level of 41…42 at.% by its magnitude (Fig. 3,a, c shows typical energy-dispersive spectra of the coatings and calculated atomic composition).

Annealing practically does not change the ratio of metal components and leads to a substantial change in content of nitrogen atoms of nitrogen and impurity oxygen atoms in the coating.

If at a low bias potential the content by nitrogen atoms is decreased by the absolute value by a value of about 2% (see Fig. 3,a,b) than in the case of large Ub = -200 V the decrease is more significant and is 5% (see Fig. 3,c,d). This can be linked with the additional formation of paths of light diffusion during the formationof solid solution of HEA atoms Mo(W) a border area as a result of radiation stimulated mixing.

The effect of bias potential and the pressure of working nitrogen atmosphere also greatly impacted on phase composition and structural state of the coatings.

Areas of X-ray diffraction spectra of the coatings, obtained under different technological conditions are shown in Fig. 4.

For comparison the spectra of the coating before the annealing and after the high temperature vacuum annealing are shown in one figure for comparison.

The analysis of the obtained diffraction spectra shows that for all deposition modes the formation of phases with cubic (fcc) lattice occurs in both layers of multilayer coatings.

In the layers of high entropy alloy it's a disordered solid solution (TiZrNbTaHf)N with the crystal lattice of NaCl type [19], in the layers of the system Mo-N it is γ-Mo2N, but in the layers of W-N it is β-W2N (PDF 25-1257). The similarity of structural states in the layers based on high entropy alloy and nitrides of VI Group transition metals (close relation of preferred orientation of crystallites layers) indicates the relationship between structure of layers and thier growth.

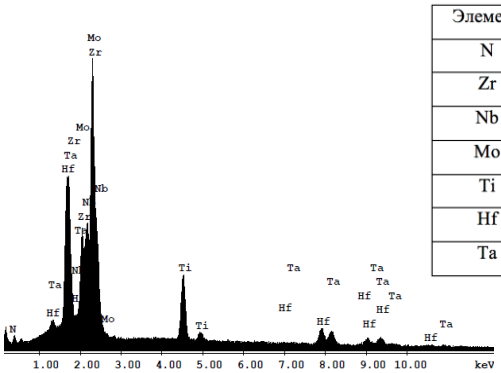

Элемент	ат. %
N	17,62
Zr	11,31
Nb	9,36
Mo	35,07
Ti	13,14
Hf	6,99
Ta	6,51

a

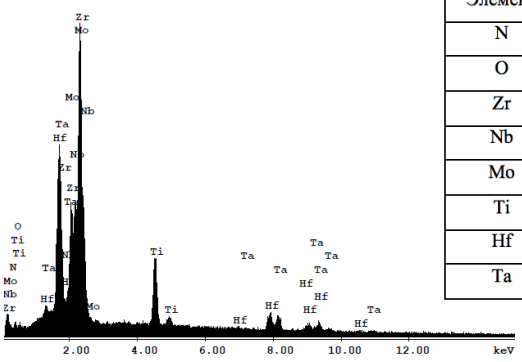

Элемент	ат. %
N	15,27
O	7,03
Zr	10,96
Nb	8,53
Mo	33,23
Ti	12,48
Hf	6,44
Ta	6,06

b

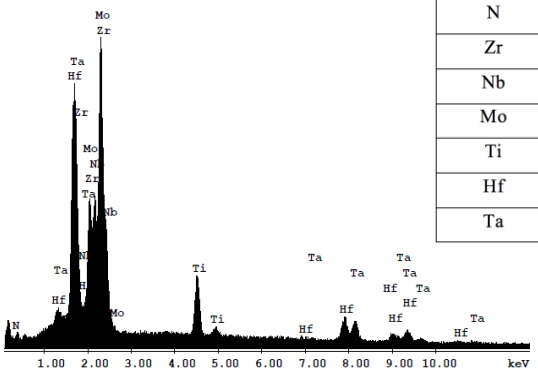

Элемент	ат. %
N	13,95
Zr	13,10
Nb	9,78
Mo	34,93
Ti	10,57
Hf	9,24
Ta	8,43

c

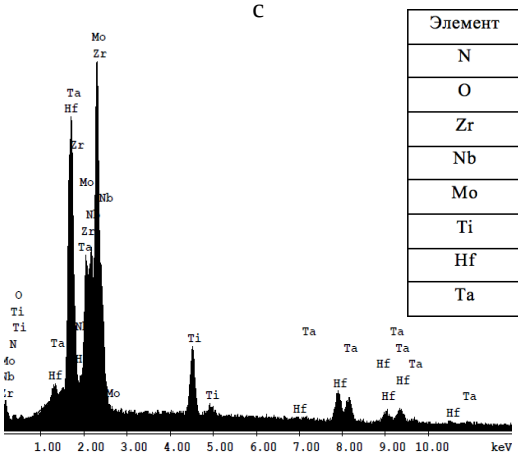

Элемент	ат. %
N	8,95
O	4,16
Zr	12,98
Nb	10,21
Mo	34,64
Ti	10,51
Hf	9,95
Ta	8,6

d

Fig. 3. Energy dispersion spectra and element contents calculated by it in the coatings (TiZrNbTaHf)N/MoN (P_N =4·10^{-3} Torr) obtained at -U_b: a – -100 V (before the annealing); b – -100 V after the annealing; c – -200 V before the annealing; d – -200 V after the annealing)

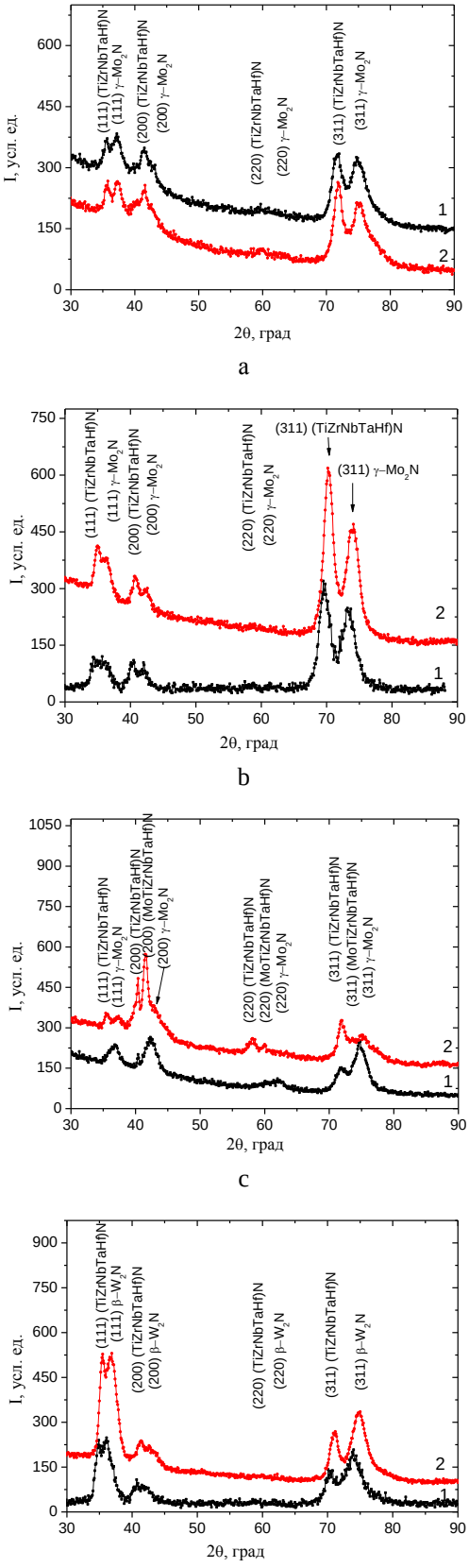

Fig. 4. Areas of X-ray diffraction spectra of the coatings (TiZrNbTaHf)N/MoN: a – P_N =1. 5·10^{-3} Torr, -U_b = 50 V; b – P_N =4·10^{-3} Torr, -U_b = 50 V; c – P_N =4·10^{-3} Torr, U_b = -200 V and d – (TiZrNbTaHf)N/WN, P_N =4·10^{-3} Torr, -U_b = 90 V. 1 – after the annealing, 2 – before the annealing at 700 ^{0}C

From the recieved spectra it can also be seen that in the coatings received during the deposition at low -Us, the postcondensation annealing does not lead to a significant change of the type of diffraction spectra (let's compare 1 and 2 on the Fig. 4,a,b,c,d). During the increase of pressure of the working nitrogen atmosphere the increase of texturating rate occurs (relative increase of intensity of reflexes). Thus, under relatively low values of -Us in the coatings of (TiZrNbTaHf)N/MoN such a texture has an axis [311] (see Fig. 4,a,b).

Applying a large negative potential Ub = -200 V leads to an increase in the degree of "chaotization" of the structure (the structure inherent to small Us is not manifested for high Us), as well as to increase of dispersion of crystalline formations in the layers of the coatings, which is manifested the most for the layers γ-Mo_2N for which with the increase of Us the average size of crystallites decreases from 54 to 37 nm. For the coatings (TiZrNbTaHf)N/WN the formation of texture with the axis [111] (see Fig.,4,d) occurs at relatively low Ub = -90 V, which is typical for the preferred minimization of deformation in the process of growth [12], the degree of perfection of which increases (spectrum 2 in Fig. 4,d) during the annealing. At the same time, reduction of the period of a lattice is observed in the annealed coatings in both layers: in (TiZrNbTaHf) N from 0.443 to 0.439 nm, and in β-W_2N layers from 0.425 to 0.421 nm.

In the coatings (TiZrNbTaHf)N/MoN annealing leads to a significant change of the lattice parameter almost exclusively in the nitride layers of high entropy alloy. The layers of Mo-N system are characterized by the slight change of the grating period remaining at a range of 0.418…0.419 nm in the coatings obtained at low $P_N = 1.5\cdot10^{-3}$ Torr and at the level of 0.425…0.424 nm at $P_N = 4\cdot10^{-3}$ Torr. An exception is the coating obtained with a large U_s = -200 V, for which even at $P_N = 4\cdot10^{-3}$ Torr grating period does not exceed 0.420 nm. One more characteristic feature of this type of the coatings is formation of nitride phases of high entropy alloy with a smaller period. So, if the main nitride phase in the layers has a period of 0.44…0.47 nm, in the case of high values of applied U_b = -200 V the formation of a new fine crystalline phase occurs. It is manifested on the diffraction spectra before the annealing in the asymmetry of reflexes (see specter 1 in Fig. 4,c), which in case of annealed coatings is found in the form of independent reflections from lattice planes of the phase with a period of 0.434…0.435 nm (see specter 2 in Fig 4,c).

Presumably this effect may be associated with the formation of mixed solid solution phase based on the high entropy nitride of the type (MoTiZrNbTaHf)N (including Mo atoms from the second layer as a compound element) on a disordered interphase border. Formation of such a layer may lead to a decrease of functional properties of the coating, and in particular – mechanical properties.

The most universal mechanical characteristics taking in account their sufficient ease of definition and good reproducibility are microindentation data and scratch testing.

The coatings of the greatest firmness according to the microidentation data are the coatings deposited at a relatively low potential bias. For the coatings (TiZrNbTaHf)N/WN the hardness reaches 44 GPa, and for (TiZrNbTaHf)N/MoN – 41 GPa.

When increasing Ub, the hardness slightly falls down to 39 GPa, apparently due to the radiation-stimulated mixing. The pressure reduction also leads to a decrease in hardness.

In the case of the coatings obtained at low $-U_b$, post-condensation annealing leads to increase of hardness of such coatings as a result of ordering at high temperatures in high entropy nitride layers [19]. To the greatest extent it affects the coatings (TiZrNbTaHf)N/WN, obtained at U_b = -90 V, where the hardness increases from 44 to 59 GPa. In the case of coatings (TiZrNbTaHf)N/MoN the largest increase in hardness is observed at U_b = -50 V: from 40.5 GPa before the annealing to 48.5 GPa after the annealing.

For the coatings obtained at high U_b = -200...-280 V the annealing is followed by a slight not only leads to increased hardness, but also accompanied by a slight drop of hardness from 39…40 GPa before the annealing to 38…37 GPa after the annealing.

The results of scratch tests also show that the greatest pressure prior to the failure is inherent to the coatings obtained at low values of Ub and for the coatings (TiZrNbTaHf)N/WN reaches the values Lc5 = 117.9 N (Fig. 5,a) and for the coatings (TiZrNbTaHf)N/MoN – Lc5 = 124.9 N (Fig. 5,b).

The annealing at 700^0C of the coatings of system (TiZrNbTaHf)N/MoN obtained at $P_N = 3 \cdot 10^{-3}$Torr, U_b = -150 V, for which the initial hardness was relatively high (35 GPa), which then increased to 41.5 GPa after the annealing led to enhanced wear resistance for all values Lc (see Table 1), and the wear is inherent to abrasion, which is manifested by the absence of large amplitude peaks (which are inherent to brittle failure) on the curve of dependence of acoustic emission on pressure (see Fig. 6,a).

Slightly larger by its magnitude hardness (48.5 GPa) of the composite coating (TiZrNbTaHf)N/MoN obtained at $P_N = 4 \cdot 10^{-3}$ Torr and U_b = -50 V after the annealing increases the critical values of LC1, LC2 and LC3 (Table 1), but at the same time the values of LC4 and LC5 are decreased, i.e. critical stresses responsible for the formation of multiple cracks and wear of material of the coating takes place.

The effect of formation of multiple cracks and brittle fracture of high hardness coating is observed even better for a steel-based substrate with a higher plasticity for the system (TiZrNbTaHf)N/WN, obtained at $P_N = 4 \cdot 10^{-3}$ Torr, U_b = -90 V, the hardness of which is increased as a result of annealing up to 59 GPa. In this case the increase of value of the critical load LC1 (Table 1) takes place only, a slight relative decrease of LC2 and LC3 and a strong decrease of LC4 and LC5. It is significant that in this area, strong peaks typical to the formation of marcoareas with brittle failure appear on the dependence of the acoustic emission signal on the load (see Fig. 6,b).

Thus, the achievement of ultrahigh hardness in a case of relatively ductile substrate may not lead to an increase in adhesive strength due to the brittle fracture of the coating during the wear in the border areas to the ductile base material.

To determine the tribological characteristics the testing scheme “ball–disc” was used in this paper, for which the balls with diameter of 6.0 mm made of sintered certified materials – Al_2O_3 and steel Ac100Cr6 were used.

Visually, friction tracks (Fig. 7) are characterized by the absence of barbs, chips, and radial cracks, which indicates the high quality of the coating and its adhesive strength.

The average width of the friction track in a case of the counterbody made of Al_2O_3 has a value of 654.88 mcm (see Fig. 7,b), and in the case of steel counterbody the track has different thickness and is characterized by a non-uniform wear pattern.

The reason for this heterogeneous nature is sticking of relatively soft and ductile metal of the counterbody to the coating, which increases the actual impact area, and further friction occurs in a pair of worn-out metal and the metal of counterbody.

Lowering of the fixed friction coefficient and increase of wear of a steel ball is also linked with this (Table 2).

Table 1

The critical load L_C for composite multilayer coatings, before and after one-hour annealing at $700\ ^0$C

Coating type	$-U_b$, V	Annealing, ^{0}C	L_C, N				
			1	2	3	4	5
(TiZrNbTaHf)N/MoN	150	-	4.52	31.8	48.2	65.8	73.1
		700	5.07	40.2	51.4	56.0	82.2
(TiZrNbTaHf)N/MoN	50	-	6.06	31.3	45.5	81.6	124.9
		700	7.33	42.8	58.4	63.8	81.7
(TiZrNbTaHf)N/WN	90	-	4.95	32.0	47.4	65.0	117.9
		700	8.31	31.3	39.7	41.3	62.7

During friction with a counterbody made of Al_2O_3 the uniform abrasive wear of the friction pair with the removal of wear products and their accumulation at the edges of the groove was observed (Fig. 7,a).

In this case, according to the data of [27], the amount of transferred material depends on the strength of adhesive bond, which depends on the electronic structure of the counterbody based on Al_2O_3 and multilayer coating, and determines the ability to form solid solutions, intermetallic compounds with each other, and oxides stable at high temperatures . This is related to the high values of the coefficient of friction during the tests with Al_2O_3 counterbody, which include high entropy nitride (TiZrHfVNbTa)N [28].

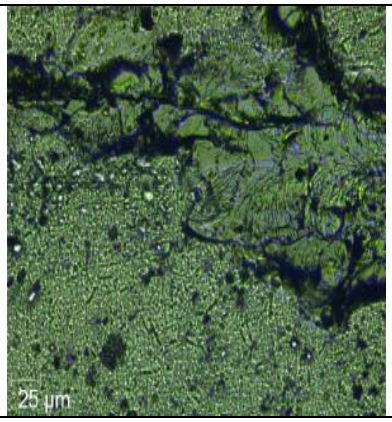

L_{c1}

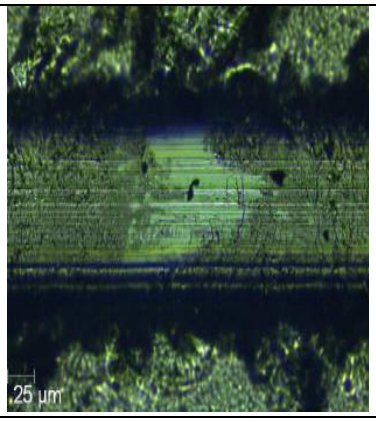

L_{c2}

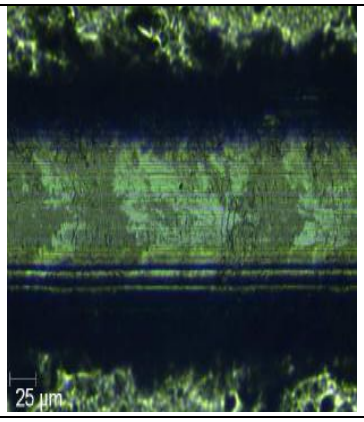

L_{c3}

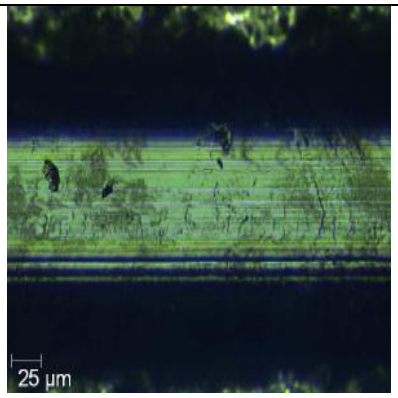

L_{c4}

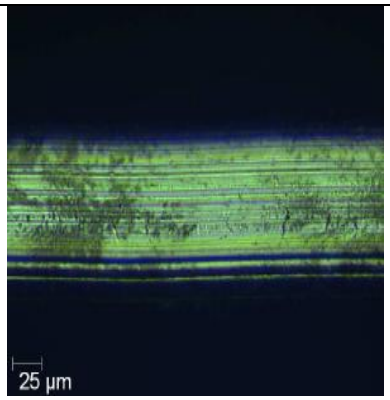

L_{c5}

L_{c1} =4.95

L_{c2} =32.0

L_{c3} =47.4

L_{c4} =65.0

L_{c5} =117.9

a

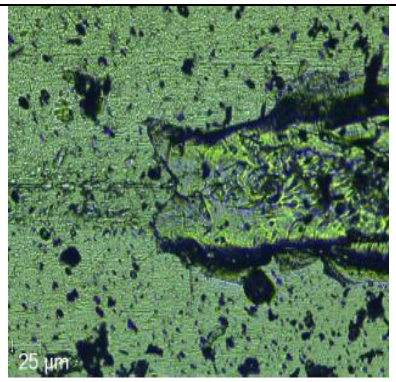

L_{c1}

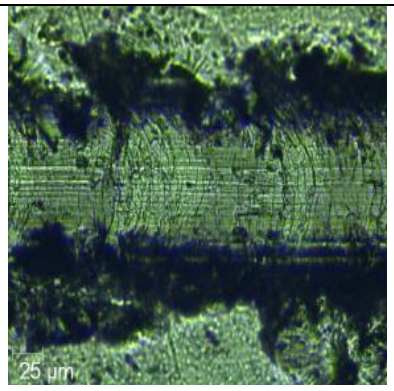

L_{c2}

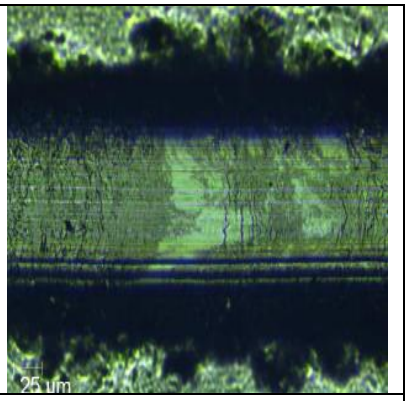

L_{c3}

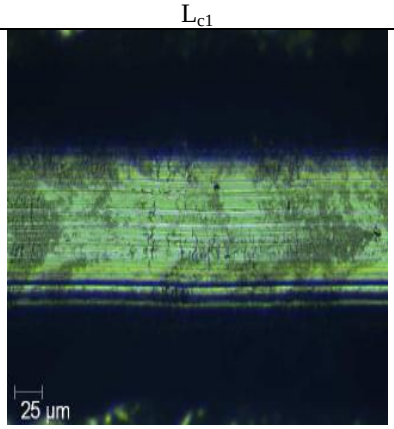

L_{c4}

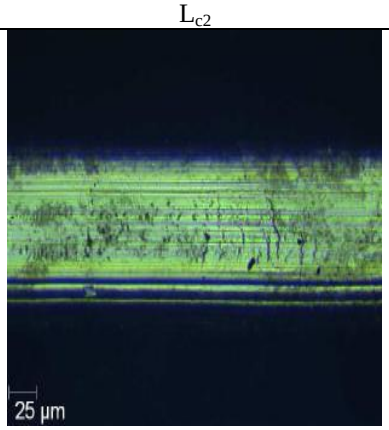

L_{c5}

L_{c1} =6.06

L_{c2} = 31.3

L_{c3} =45.5

L_{c4} =81.6

L_{c5} =124.9

b

Fig. 5. View of wear tracks and the resulting critical loads for the coatings:
a – (TiZrNbTaHf)N/MoN (P_N =4·10^{-3}Torr, U_b = -150 V)
and b – (TiZrNbTaHf)N/WN (P_N =4·10^{-3} Torr, U_b = -90 V)

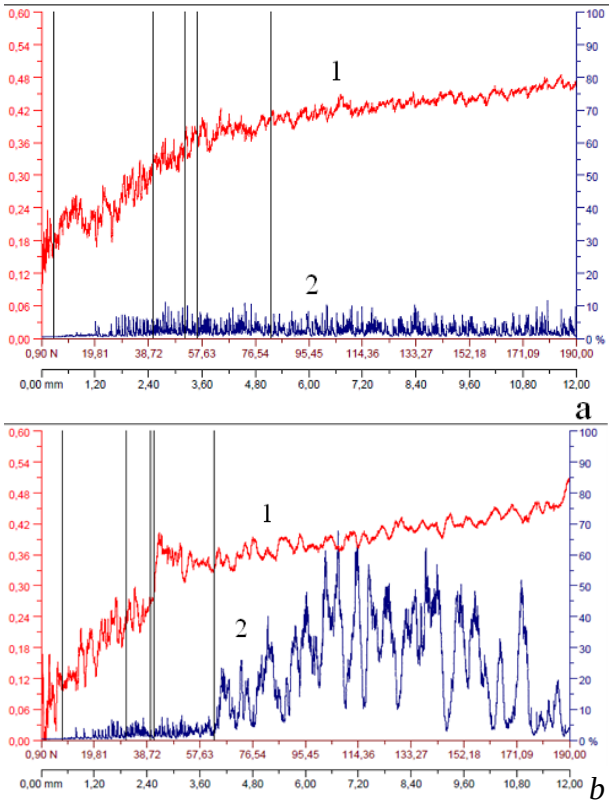

Fig. 6. Changes in average values of the coefficient of friction (spectrum 1, left scale) and in the amplitude of acoustic emission (spectrum 2, right scale) for the coatings: a - (TiZrNbTaHf)N/MoN (P_N =4·10^{-3} Torr, U_S = -150 V) and b – (TiZrNbTaHf)N/WN (P_N =4·10^{-3} Torr, U_b = -90 V)

At the same time the coatings possess good wear resistance: wear value for both types of counterbodies is within the limit (0.39…2.12)×10^{-5} mm^3×N^{-1}×mm^{-1}. Wear of the counterbody of Al_2O_3 is also sufficiently small – 2.25×10^{-6}mm^3×N^{-1}×mm^{-1} (Table 2), in contrast with a steel counterbody Ac100Cr6 for which wear differs by one order and has a value of 2.59×10^{-4} mm^3×N^{-1}×mm^{-1}.

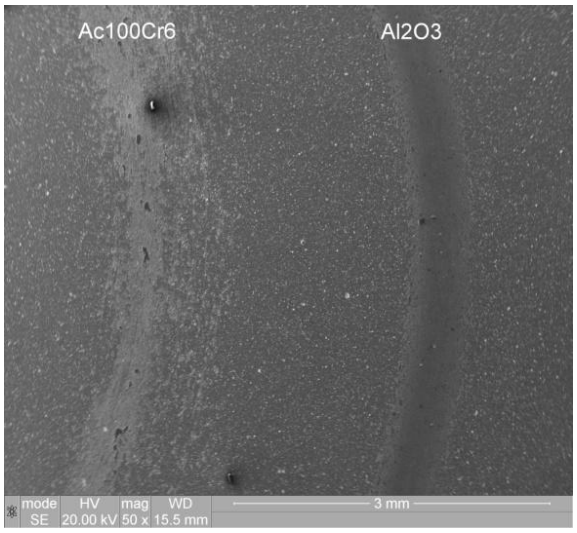

a

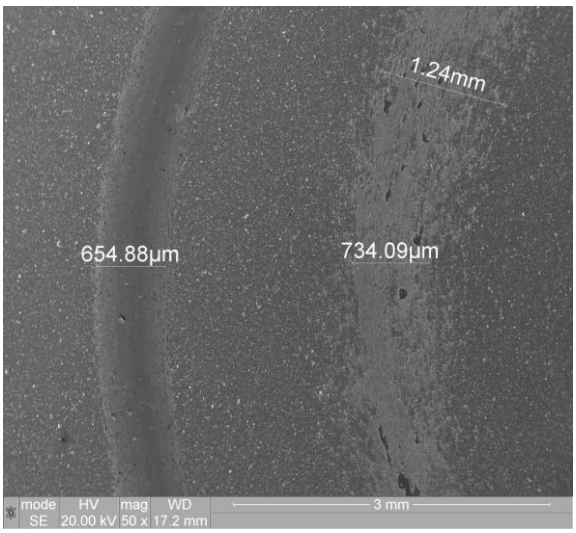

b

Fig. 7. Images of friction tracks during the tests (by "ball – disc" scheme with a counterbody (ball) made of Al_2O_3 and steel Ac100Cr6) of the multilayer coating (TiZrNbTaHf)N/MoN (P_N = 4·10^{-3} Torr, U_b = -50 V): a – with detailed friction tracks by the type of the counterbody, b – with the determined average sizes of friction tracks for different counterbodies

Table 2

The tribological characteristics of the multilayer coating (TiZrNbTaHf)N/ MoN (P_N = 4×10^{-3} Torr, U_b = -50V) during the tests by the scheme "ball – disc" with counterbody (ball) of Al_2O_3 and steel Ac100Cr6

Type of counterbody	Coefficient of friction	Wear factor, mm^3×N^{-1}×mm^{-1}	
		Counterbody	Coated samples
Al_2O_3	0.83	2.25×10^{-6}	3.90×10^{-6}
Ac100Cr6 steel	0.57	2.59×10^{-4}	2.12×10^{-5}

Thus, a quite universal resistance of multilayer coatings based on nitrides of high entropy alloys to various types of counterbodies, different in hardness and toughness opens good perspectives to use such coatings as protective coatings at complex exposures in conditions of abrasive wear [29, 30].

The study was conducted in the CCU, agreement No.14.594.21.0010 and unique works identifier RFMEFI62114X0005 (under the support of the Ministry of Education of Russia).

The work was performed as part of comprehensive state-funded research 0113U001079, funded by the Ministry of Education and Science of Ukraine.

REFERENCES

1. А. Кавалейро, Д. де Хоссон. Наноструктурные покрытия // *Техносфера*. 2011, 752 с.

2. A.D. Pogrebnjak, A.P. Shpak, N.A. Azarenkov, V.M. Beresnev. Structure and properties of hard and superhard nanocomposite coatings // *Phys.-Usp.* 2009, v. 52, N 1, p. 29-54.

3. J.M. Lackner, W. Waldhauser, L. Major, J. Morgiel, M. Kot, B. Major. Nanocrystalline Cr/CrN

and Ti/TiN multilayer coatings produced by pulsed laser deposition at room temperature // *Bulletin of the Polish Academy of Sciences Technical science*s. 2006, v. 54, N 2, p. 175-180.

4. K.J. Kadhim, N. Abd Rahman, M.R. Salleh, K.I. Mohd Zukee. Effects of Layer Thickness on the Microstructures of TiN/AlTiN Multilayer Coatings // *Applied Mechanics and Materials*. 2015, v. 761, p. 417.

5. K. Lukaszkowicz, L.A. Dobrzański, A. Zarychta, L. Cunha. Mechanical properties of multilayer coatings deposited by PVD techniques onto the brass substrate // *Journal of Achievements in Materials and Manufacturing Engineering*. 2006, v. 15, issue 1-2, p. 47-52.

6. W. Kwaśny, L.A. Dobrzański, M. Król, J. Mikuła. Fractal and multifractal characteristics of PVD coatings // *Journal of Achievements in Materials and Manufacturing Engineering.* 2007, v. 24, issue 2, p. 159-162.

7. C. Harish Barshilia, Anjana Jain, K.S. Rajam. Structure, hardness and thermal stability of nanolayered TiN/CrN multilayer coatings // *Vacuum.* 2004, v. 72, p. 241-248.

8. Zhang Guo-Ping, Wang Xing-Quan, Lu Guo-Hua, et al. Effect of pulsed bias on the properties of ZrN/TiZrN films deposited by a cathodic vacuum arc // *Chin. Phys. B*. 2013, v. 22, N 3, p. 035204 (5).

9. Z. Zhang, O. Rapaud, N. Allain, et al. Characterizations of Magnetron Sputtered CrSiN/ZrN Multilayer Coatings–from Structure to Tribological Behaviors // *Advanced Engineering Materials.* 2009, v. 11, issue 8, p. 667-673.

10. V.M. Beresnev, O.V. Sobol', A.D. Pogrebnjak, P.V. Turbin, S.V. Litovchenko. Thermal stability of the phase composition, structure, and stressed state of ion-plasma condensates in the Zr-Ti-Si-N system // *Technical Physics*. 2010, v. 55, N 6, p. 871-873.

11. O.V. Sobol'. Control of the Structure and Stress State of thin films and coatings in the process of their preparation by ion-plasma methods // *Physics of the Solid State*. 2011, v. 53, N 7, p. 1464-1473.

12. O.V. Sobol', A.A. Andreev, S.N. Grigoriev, V.F. Gorban', et al. Effect of high-voltage pulses on the structure and properties of titanium nitride vacuum-arc coatings // *Metal Science and Heat. Treatment*. 2012, v. 54, N 3-4, p. 195-203.

13. V. Dolique, A-L. Thomann, P. Brault, et al. Complex structure/composition relationship in thin films of AlCoCrCuFeNi high entropy alloy // *Materials Chemistry and Phys.* 2009, v. 117, issue 1, p. 142-147.

14. V. Dolique, A.-L. Thomann, P. Brault, et al. Thermal stability of AlCoCrCuFeNi high entropy alloy thin films studied by in-situ XRD analysis // *Surface and Coatings Technology*. 2010, v. 204, p. 1989-1992.

15. Ming-Hung Tsai, Chun-Wen Wang, Che-Wei Tsai, et al. Thermal Stability and Performance of NbSiTaTiZr High-Entropy Alloy Barrier for Copper Metallization // *Journal of The Electrochemical Society*. 2011, v. 158 (11), p. 1161-1165.

16. S. Ranganathan. Alloyed pleasures: Multimetallic cocktails // *Current Science*. 2003, v. 85, N 10, p. 1404-1406.

17. R. Krause-Rehberg, A.D. Pogrebnyak, V.N. Borisyuk, et al. Analysis of local regions near interfaces in nanostructured multicomponent (Ti-Zr-Hf-V-Nb)N coatings produced by the cathodic-arc-vapor-deposition from an arc of an evaporating cathode // *The Physics of Metals and Metallography*. 2013, v. 114, issue 8, p. 672-680.

18. A.D. Pogrebnjak, V.M. Beresnev, D.A. Kolesnikov, et al. Multicomponent (Ti-Zr-Hf-V-Nb)N Nanostructure Coatings Fabrication, High Hardness and Wear Resistance // *Acta Physica Polonica, A.* 2013, v. 123, issue 5, p. 816.

19. O.V. Sobol', A.A. Andreev, V.F. Gorban', et al. Reproducibility ofthe single-phase structural state of the multielement high entropy Ti-V-Zr-Nb-Hf system and related superhard nitrides formed by the vacuum-arc method // *Tech. Phys. Lett.* 2012, v. 38, N 7, p. 616-619.

20. J.M. Lackner, W. Waldhauser, L. Majo, M. Kot. Tribology and Micromechanics of Chromium Nitride Based Multilayer Coatings on Soft and Hard Substrates // *Coatings.* 2014, v. 4, p. 121-138.

21. M.K. Samani, X.Z. Ding, N. Khosravian, et al. Thermal conductivity of titanium nitride/titanium aluminum nitride multilayer coatings deposited by lateral rotating cathode arc // *Thin Solid Films*. 2015, v. 578, p. 133-138.

22. A.R. Henriques, O.C. Schichi, E.T. Galvani. Microstructural characterization of TiN/ZrN multilayer coatings on titanium alloy produced by powder metallurgy // *Tecnol. Metal. Mater. Miner*. 2014, v. 11, N 3, p. 195-201.

23. Н.А. Азаренков, О.В. Соболь, В.М. Береснев и др. Вакуумно-плазменные покрытия на основе многоэлементных нитридов // *Металлофизика и новейшие технологии.* 2013, т. 35, №8, с. 1061-1084.

24. А.А. Андреев, Л.П. Саблев, С.Н. Григорьев. *Вакуумно-дуговые покрытия*. Харьков: ННЦ ХФТИ, 2010, 318 с.

25. L.S. Palatnik, M.Ya. Fuks, V.M. Kosevich. *Mechanism of formation and substructure of condensed films*. M.: "Nauka", 1972, 320 p.

26. И.Д. Ибатуллин. *Кинетика усталостной повреждаемости и разрушения поверхностных слоев:* Монография. Самара: Самарский государственный технический университет, 2008, 396 с.

27. Н.К. Мышкин, М.И. Петроковец. *Трение, смазка, износ. Физические основы и технические приложения трибологии*. М.: ФИЗМАТЛИТ, 2007, 368 с.

28. S.N. Grigoriev, O.V. Sobol', V.M. Beresnev, et al. Tribological characteristics of (TiZrHfVNbTa)N coatings applied using the vacuum arc deposition method // *Journal of Friction and Wear September*. 2014, v. 35, issue 5, p. 359-364.

29. A.D. Pogrebnjak and V.M. Beresnev. *Nanocoatings Nanosystems Nanotechnologyes*. USA: Bentham Sci. Publ., 2012, 147 p.

30. A.D. Pogrebnjak, O.V. Bondar, N.K. Erdybaeva, S.V. Plotnikov, P.V. Turbin, S.S. Grankin, V.A. Stolbovoy, O.V. Sobol', D.A. Kolesnikov, C. Kozak. Influence of thermal annealing and deposition conditions on structure and physical-mechanical properties of multilayered nanosized TiN/ZrN coatings // *Przeglad Elektrotechniczny.* 2015, N 12, p. 228-233.

Article received 01.10.2015

СТРУКТУРА И МЕХАНИЧЕСКИЕ СВОЙСТВА НИТРИДНЫХ МНОГОСЛОЙНЫХ СИСТЕМ НА ОСНОВЕ ВЫСОКОЭНТРОПИЙНЫХ СПЛАВОВ И ПЕРЕХОДНЫХ МЕТАЛЛОВ VI ГРУППЫ

У.С. Немченко, В.М. Береснев, О.В. Соболь, С.В. Литовченко, В.А. Столбовой, В.Ю. Новиков, А.А. Мейлехов, А.А. Постельник, М.Г. Ковалева

Проанализировано влияние технологических параметров получения на возможности структурной инженерии и механические свойства многослойных композиций из слоев нитридов высокоэнтропийных сплавов Ti-Zr-Nb-Ta-Hf и нитридов переходных металлов VI группы. Показано, что при потенциале смещения Us менее -150 В, подаваемом на подложку при осаждении, в многослойных покрытиях с толщиной слоев около 50 нм можно достичь двухфазного состояния с преимущественной ориентацией кристаллитов, что обуславливает высокую твердость (до 44 ГПа) и одновременно высокую адгезионную прочность (критическая нагрузка до 125 Н), а также низкий износ (как с контртелом Al_2O_3, так и со сталью Ac100Cr6). Высокотемпературный отжиг (700 ^{0}C) таких покрытий приводит к усилению текстуры в результате атомарного упорядочения, что сопровождается ростом твердости до 59 ГПа. Подача потенциала смещения, превышающего 150 В, сопровождается существенным перемешиванием на межфазной границе, что приводит к разориентации и повышению дисперсности кристаллитов, уменьшению твердости и износостойкости. Высокотемпературный отжиг таких структур приводит к снижению механических свойств.

СТРУКТУРА І МЕХАНІЧНІ ВЛАСТИВОСТІ НІТРИДНИХ БАГАТОШАРОВИХ СИСТЕМ НА ОСНОВІ ВИСОКОЕНТРОПІЙНИХ СПЛАВІВ І ПЕРЕХІДНИХ МЕТАЛІВ VI ГРУПИ

У.С. Немченко, В.М. Береснєв, О.В. Соболь, С.В. Литовченко, В.А. Столбовий, В.Ю. Новіков, А.А. Мейлєхов, А.А. Постельник, М.Г. Ковальова

Проаналізовано вплив технологічних параметрів отримання на можливості структурної інженерії та механічні властивості багатошарових композицій з шарів нітридів високоентропійних сплавів Ti-Zr-Nb-Ta-Hf і нітридів перехідних металів VI групи. Показано, що при потенціалі зміщення Us менше -150 В, що подається на підкладку при осадженні, у багатошарових покриттях з товщиною шарів близько 50 нм можна досягти двофазного стану з переважною орієнтацією кристалітів, що обумовлює високу твердість (до 44 ГПа) і одночасно високу адгезійну міцність (критичне навантаження до 125 Н), а також низький знос (як з контртілом Al_2O_3, так і зі сталлю Ac100Cr6). Високотемпературний відпал (700 °C) таких покриттів призводить до посилення текстури в результаті атомарного упорядкування, що супроводжується зростанням твердості до 59 ГПа. Подача потенціалу зміщення, що перевищує 150 В, супроводжується істотним перемішуванням на міжфазній межі, що призводить до розорієнтації і підвищення дисперсності кристалітів, зменшення твердості і зносостійкості. Високотемпературний відпал таких структур призводить до зниження механічних властивостей.